
Article:
Torelli, G. and Lees, J.M. (2020) Interface bond strength of lightweight low-cement functionally layered concrete elements. Construction and Building Materials, 249. 118614. ISSN 0950-0618

https://doi.org/10.1016/j.conbuildmat.2020.118614

Interface bond strength of lightweight low-cement functionally layered concrete elements

Citation:
Torelli, G. and Lees, J. M. (2020) 'Interface bond strength of lightweight low-cement functionally layered concrete elements', Construction and Building Materials. Elsevier, 249, p. 118614. doi: 10.1016/J.CONBUILDMAT.2020.118614.

Version:
Accepted for publication

Interface bond strength of lightweight low-cement functionally layered concrete elements

Giacomo Torelli[1*], Janet M Lees[2]

[1] Department of Civil and Structural Engineering, University of Sheffield, Sheffield, S1 3JD, UK

[2] Department of Engineering, University of Cambridge, Cambridge, CB2 1PZ, UK

*Corresponding author, E-mail: g.torelli@sheffield.ac.uk

Abstract

Production of cement accounts for around 5% of human-made carbon emissions. When the selection of a cement-intensive mix with low porosity is driven by durability requirements, the resulting low permeability of the material is only fully exploited in peripheral regions of the element where the material acts as a physical barrier against the penetration of aggressive substances. This paper explores the potential of casting layered prismatic elements composed of an external durability layer and a lightweight core section as a means to achieve cement and weight savings. Layered elements are traditionally obtained by casting new concrete layers onto already hardened older concrete layers. A major problem with this technique is that planes of weakness are obtained at the interfaces between the layers. The bond between the layers can be improved by casting the materials at approximately the same time. However, research to date has not yet demonstrated the viability of producing elements with wet cast external layers. Furthermore, the effects of delays between successive pours on the mechanical tensile performance of the interfaces in layered elements have not been quantified. An original method is presented to form prismatic elements composed of an external durability layer and a lightweight core section by casting two concrete mixes at approximately the same time. The approach is validated by realising a proof-of-concept prototype layered element. A set of additional layered elements are cast with various pour delays and cored across the interface between their layers to characterize the interlayer bond strength by direct tension. To interpret the mechanisms affecting the bond, the variation of tensile bond strength with the location of the sample and the impact of roughness are also investigated. When the pour delay was minimal, failure did not occur at the interlayer. The relationship between pour delay and bond strength is markedly nonlinear, with bond strength reductions of more than 30% for pour delays of only three hours. It was also found that the bond strength of the interface varies significantly with the considered location and that up to 40% of the bond strength reduction due to a delay between the castings can be recovered by roughening the surface of the older concrete prior to casting the newer mix. The successful realisation of wet cast prismatic elements with an external durability layer is an important step towards the realisation of light-weight layered concrete elements with low embodied energy.

Keywords

Concrete; Fresh concrete; Rheology; Multilayer casting; Formwork; Interface; Bond strength.

1 Introduction

The industrial production of cement, the main ingredient of concrete, is responsible for about 5 % of the global carbon emissions [1]. Hence, there is an urgent need to develop technologies aimed at minimising the use of cement in concrete structures. Experimental evidence has shown that material savings of up to 40 % can be achieved while preserving structural strength by designing functionally layered elements, i.e. composite concrete members composed of layers of different concrete mixes [2–5]. Functional layering allows mixes with high cement contents to be placed only where they contribute to one or multiple functions of the element, thereby allowing for significant cement savings in other areas. Furthermore, lightweight mixes can be used in the regions where high-density mixes are not needed, thereby minimising the overall weight of a structural element. Consequently, dead loads are reduced, more slender elements are designed, and less material is consumed. The aim of this paper is twofold. First, to establish a design concept, based on the idea of functional layering, to reduce both the cement content and the self-weight of precast concrete beams when the mix selection is driven by durability requirements. Secondly, to develop a suitable production process for lightweight low-cement functionally layered elements and to investigate the effects of delays between successive pours on the bond between different concrete mixes.

When the selection of a concrete mix with high cement content is driven by durability requirements, the low permeability of the material is only fully exploited in peripheral regions of the element where the material acts as a physical barrier against the penetration of aggressive substances. The penetration of fluids and gases can be delayed by minimizing the concrete permeability, extent of cracking and crack widths [6,7]. The permeability of the material is generally limited by selecting cement-intensive mixes characterised by low-porosity. High-cement-content strain-hardening Engineered Cementitious Composites (ECCs) can also be designed to minimize the extent of cracking and crack widths [8–10]. These approaches mitigate the ingress of chlorides or CO_2 [6,11] and reduce the propensity for the corrosion of internal steel reinforcement. However, in a structural element with a homogeneous concrete composition the durability requirements then dictate the cement content throughout. The present work explores functional gradation for cement reduction in prismatic pre-cast concrete beams. Low-permeability cement-intensive mixes are used only in external exposed layers

to ensure the overall durability performance of the element. High-porosity lightweight materials with lower cement contents are then assigned to core areas to achieve substantial cement and weight savings.

Consider as an example a precast concrete beam designed to act compositely with a floor slab [12] (see Figure 1a). To protect the steel reinforcement against the ingress of aggressive materials through the bottom and lateral surfaces, a composite section with a relatively low-porosity U-shaped external protective layer and a core of relatively high-porosity material can be designed (see Figure 1b). In Figure 1b, the relatively low- and high-porosity materials are denoted as A and B respectively. The cement savings S_C and weight savings S_w compared to a homogeneous beam of low-porosity material (Figure 1a) can be expressed as:

$$S_C = \frac{C_{hom} - C_{lay}}{C_{hom}} = \frac{c_A - c_B}{c_A} \frac{A_I}{A_T} \tag{1-1}$$

$$S_W = \frac{W_{hom} - W_{lay}}{W_{hom}} = \frac{\rho_A - \rho_B}{\rho_A} \frac{A_I}{A_T} \tag{1-2}$$

where C_{hom} and C_{lay} are the cement contents per unit length (expressed, for example, in kg m^{-1}) in the homogeneous beam and in the layered beam respectively, c_A and c_B are the cement contents per unit volume (expressed, for example, in kg m^{-3}) of Material A and Material B respectively, A_I and A_T are the cross-sectional areas of the internal core and of the entire composite section respectively, W_{hom} and W_{lay} are the weight per unit length of the homogeneous beam and of the layered beam respectively, and ρ_A and ρ_B are the mass-densities of Material A and Material B respectively. The cement and weight savings are directly proportional to the ratio between the area of the core section and total area of the composite section.

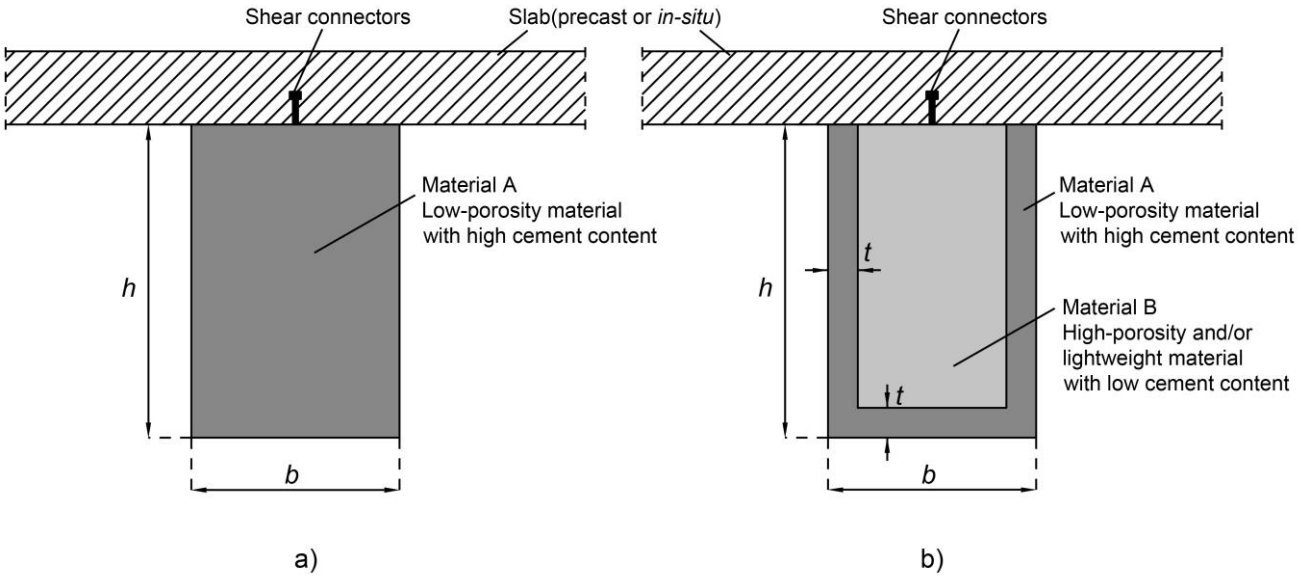

Figure 1 Prismatic pre-cast concrete beams: (a) typical cross-section with homogeneous concrete composition and (b) functionally layered beam section with a low-porosity U-shaped external protective layer.

Two virtual materials, denoted as A and B1, were designed according to the BRE mix design method [13] to explore the potential to save cement by using mixes with a low water/cement ratio only in the external layers. A minimum compressive strength of 35 MPa was assumed. Water/cement ratios of 0.40 and 0.60 were selected resulting in cement contents of 450 and 300 kg m^{-3} for materials A and B1 respectively. This resulted in a relatively low-porosity cement-intensive protective external layer. An additional virtual material, denoted as B2, was designed using the mix proportions of material B1 as a baseline and substituting traditional quarried aggregates with lightweight aggregates that are 50 % lighter. The design parameters, design density and strength of the virtual materials A, B1 and B2 are reported in Table 1. With reference to the geometric parameters defined in Figure 1b and assuming a height to breadth ratio h/b of 2, the cement and weight savings as a function of the beam height h for thicknesses t of the external layer in the range of 30 – 50 mm, are plotted in Figure 2a and Figure 2b respectively. Figure 2a shows that, for the considered parameters, cement savings of more than 25 % may be achieved by selecting a low water/cement ratio for the external layer only. Greater savings are generally obtained for larger beams, where the core area represents a larger portion of the total cross-sectional area. Figure 2b shows that weight savings of more than 30 % can be achieved through functional layering. Varying the thickness t of the external layer in the range between 50 mm and 30 mm has an impact in terms of both the cement and weight savings e.g. reducing t from 50 to 30 mm allows the relative cement savings to be increased by up to around 50 %.

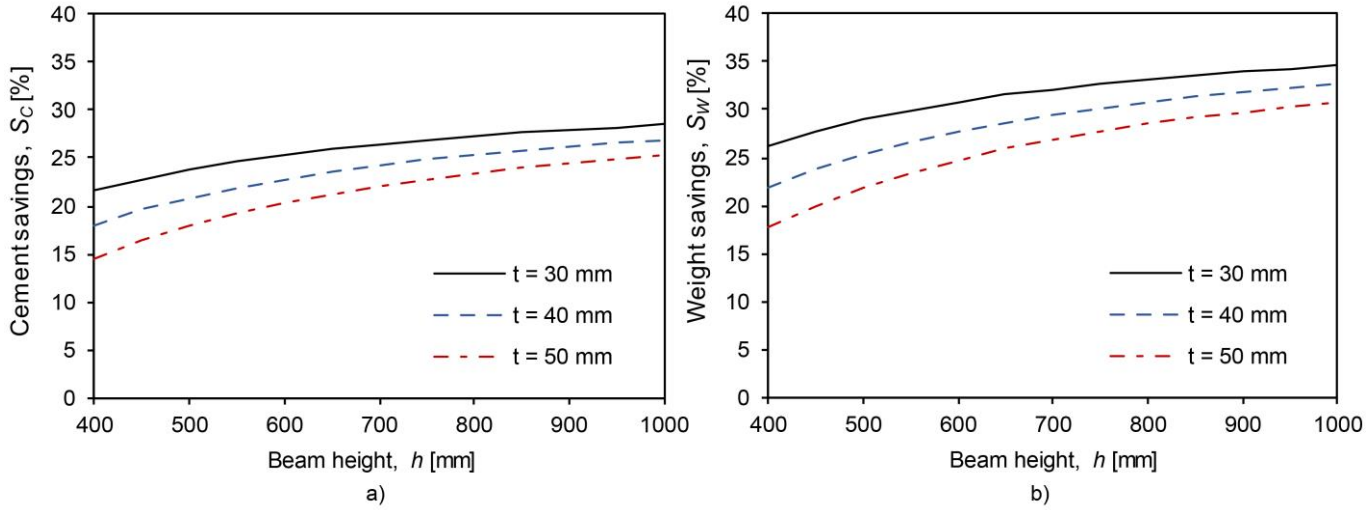

Figure 2 Potential cement and weight savings for a beam with height h for various values of thickness t of the external layer, assuming h/b=2: (a) Percentage of cement savings S_C using Materials A and B1, and (b) Percentage of weight savings S_W for Materials A and B2.

Table 1 Mix compositions, design density and strength of the virtual materials A, B1 and B2.

Parameter	**Unit**	**Material A**	**Material B1**	**Material B2**
Cement CEM I	[kg m^{-3}]	714	385	385
Water	[kg m^{-3}]	250	250	250
Sand 0/4 mm	[kg m^{-3}]	913	1286	-
Gravel 4/10 mm	[kg m^{-3}]	468	350	-
Lightweight sand 0/4 mm	[kg m^{-3}]	-	-	643
Lightweight gravel 4/10 mm	[kg m^{-3}]	-	-	175
Design density ρ	[kg m^{-3}]	2345	2271	1453
Design compressive strength f_C	[MPa]	70	33	33

Functionally layered elements can either be produced by sequentially adding new layers when the existing ones have already set and hardened or by casting multiple mixes at approximately the same time. These two techniques are referred to as fresh-on-hardened and fresh-on-fresh casting respectively [5]. Fresh-on-hardened casting methods are relatively well-developed owing to their widespread use in the precast industry, where precast concrete elements are combined with additional layers cast in situ to enhance strength and durability. Common applications include bridge decks with topping layers [14,15], structural connections between precast elements [16] and precast U-shaped shell units within which a different concrete mix is cast in situ [17].

However, a major problem with fresh-on-hardened casting is that a surface of weakness, commonly referred to as *cold joint*, is generally obtained at the interface between different concrete layers [5,18,19]. The adhesion

between newer and older concrete layers strictly depends on the workmanship and cleanliness of the interface on pouring. Owing to the variability in the quality control on construction sites, the effectiveness of the bond can be limited. An additional factor limiting the adhesion between layers is differential shrinkage. In common concrete mixes, most of the drying shrinkage contraction generally occurs within the first few months after casting [9]. Thus, in practical fresh-on-hardened applications involving long times between pours, gradual shrinkage contractions develop in the new layers that are restrained by the older concrete. Consequently, tensile stresses and associated micro-cracks may develop in the proximity of the interface that can potentially reduce its load carrying capacity. Hence, the interface between new and old concrete layers is generally weaker than either of the two materials [20,21].

The effectiveness of the interlayer bond in functionally layered elements can potentially be improved through fresh-on-fresh casting, i.e. by casting the layers at the same time or sequentially with a relatively short delay [5]. When multiple layers are mixed and cast within relatively short time, the different materials can intermix, hydration reactions can take place across the interfaces and a chemical bond can develop between the layers. A further practical advantage of using fresh-on-fresh casting is the potential for significant reduction in manufacturing time.

Existing experimental studies on the effects of pour delays on the mechanical performance of cold joints have primarily focussed on structural elements with homogeneous concrete composition. When, for example, two concrete batches are required to realise a relatively large structural element and the pour of the second batch is delayed, the initially poured batch might have started to set at the time of the second pour [9]. Consequently, effective knitting together of the two batches of concrete through vibration might not be possible and the interface between the two batches is a potential cold joint [22–24]. Owing to difficulties in achieving good compaction, small voids and relatively high porosity might be expected in the proximity of the interface that locally increase the permeability to aggressive substances [24]. Thus, pour delays play a critical role in the structural behaviour and mass transport mechanisms of homogeneous concrete elements.

However, research to date has not yet studied the effects of delays between successive pours on the mechanical performance of the interfaces in functionally layered elements. This knowledge is urgently needed to inform design and production processes for tailored structural elements, thereby enabling safe realisation of optimised, low-carbon concrete structures.

This work makes a fundamental contribution to research on functionally layered concrete by demonstrating the feasibility of fresh-on-fresh prismatic structural elements with durability layers and studying for the first time the effects of delays between successive pours on the bond between different concrete mixes. The original fresh-on-fresh casting method is based on the use of temporary vertical panels to produce layered concrete elements composed of i) an external U-shaped layer of low-permeability concrete with high cement content and ii) a section core of lightweight concrete with low cement content (see Figure 1b). The method is validated by realising a prototype prismatic U-layer element that represents a proof-of-concept for future production. Additional elements are cast with pour delays of up to 48 hours to establish the relationship between pour delay and interface bond strength. The interface bond strength of each element is characterised by coring cylindrical samples across the interface and testing them in direct tension. To interpret the mechanisms affecting the bond, the variation of bond strength with the location of the sample and the impact of roughness are also investigated.

2 Production method

A major challenge in the adoption of fresh-on-fresh casting methods is the control of the fresh state deformations of the layers. When layers of different materials are cast within the same mould, material density differentials may result in shear stresses that cause the heavier materials to flow underneath the lighter ones [5,25]. In the present work, this phenomenon is referred to as global instability in the fresh state [5]. A plausible instability for a composite section with an external U-shaped layer of relatively heavy material is represented in Figure 3. If excessive fresh-state deformations occur, a spatial distribution of material composition is obtained that differs from the one envisioned in the design. Hence, limiting the fresh-state deformations of the layers is crucial to control the hardened-state properties of layered concrete elements. Production processes and fresh-state properties of the concrete mixes must thus be suitably designed to limit the fresh-state deformations of layered concrete elements.

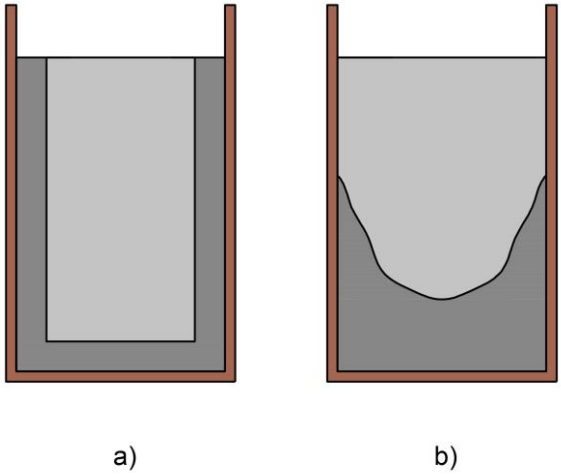

Figure 3 Schematic representation of the fresh state deformations of layered section with an external U-shaped layer of relatively heavy material: (a) stable and (b) unstable behaviour.

In the fresh state, concrete behaves as a yield stress fluid, that is, a material that exhibits solid behaviour for low shear stresses and starts to flow when a threshold shear stress is exceeded [26–28]. This threshold shear stress, referred to as yield stress, depends on a number of factors including mix composition, time-dependent chemical and physical reactions, and temperature [28–31]. When cast in conventional moulds, concrete must be able to flow to fill all the voids. If stiff mixes with a limited ability to flow are cast, air is generally entrapped in the form of large voids. Vibration is thus applied to fluidise the concrete and permit the entrapped air to rise to the surface. Indeed, vibration allows the yield stress of the material to be temporarily lowered [32,33]. However, the amount of applied vibration must be limited as excess vibration may result in local instability phenomena such as bleeding and segregation [29]. Mixes that require vibration to achieve good compaction are commonly referred to as Conventional Vibrated Concrete (CVC). If, by contrast, the material is fluid enough to flow under its own weight, good compaction is achieved without applied vibration. In this case, the material is referred to as Self-Compacting Concrete (SCC). Vibration of SCC should be avoided as the inherently low yield-stress of the material makes it particularly prone to bleeding and segregation.

In the case of functionally layered elements, production processes and rheological properties of the materials must meet additional requirements. Fluidity of the mixes and vibration must be limited to reduce the fresh state deformations. For this reason, most experimental studies on functionally layered concrete focused on the use of CVC with limited or no vibration [2–4,8,34–38]. However, a major problem with these production methods is the difficulty in achieving good compaction while controlling the fresh state deformations. Indeed, poor compaction is generally obtained in the absence of vibration. On the other hand, difficulties arise in controlling

the fresh state deformations with confidence if vibration is applied. This is because visual inspection of the deformations at the core of an element is generally impossible. Furthermore, the complex interaction between such factors as frequency, amplitude, acceleration and radius of action of the vibrator make it particularly difficult to assess effects of vibration on the rheological properties of the mixes and thus on the fresh state deformations of the element [28].

An original fresh-on-fresh casting method that combines the use of CVC and SCC is adopted here to achieve good compaction and limit the fresh state deformations of layered concrete elements composed of an external U-shaped layer and a rectangular core section. CVC is used for the external layer to provide the necessary stiffness to limit the fresh state deformations of the layered system. The layer is cast and fully compacted with the aid of removable panels that demarcate its shape on casting and vibration (see Figure 4a). SCC is then poured within the core section (Figure 4b) and the panels are removed (Figure 4c). The use of SCC ensures adequate compaction of the core section without vibration, thereby eliminating the associated difficulties in controlling the fresh state deformations of the layered element. The proposed fresh-on-fresh casting method represents a proof-of-concept for future production of reinforced layered elements. Indeed, unreinforced layered elements are cast through the aid of temporary panels that would not interfere with possible reinforcement cages pre-placed in the core sections. Furthermore, the flowability of SCC makes the method suitable to cast reinforced layered concrete elements with a congested reinforcement in the core.

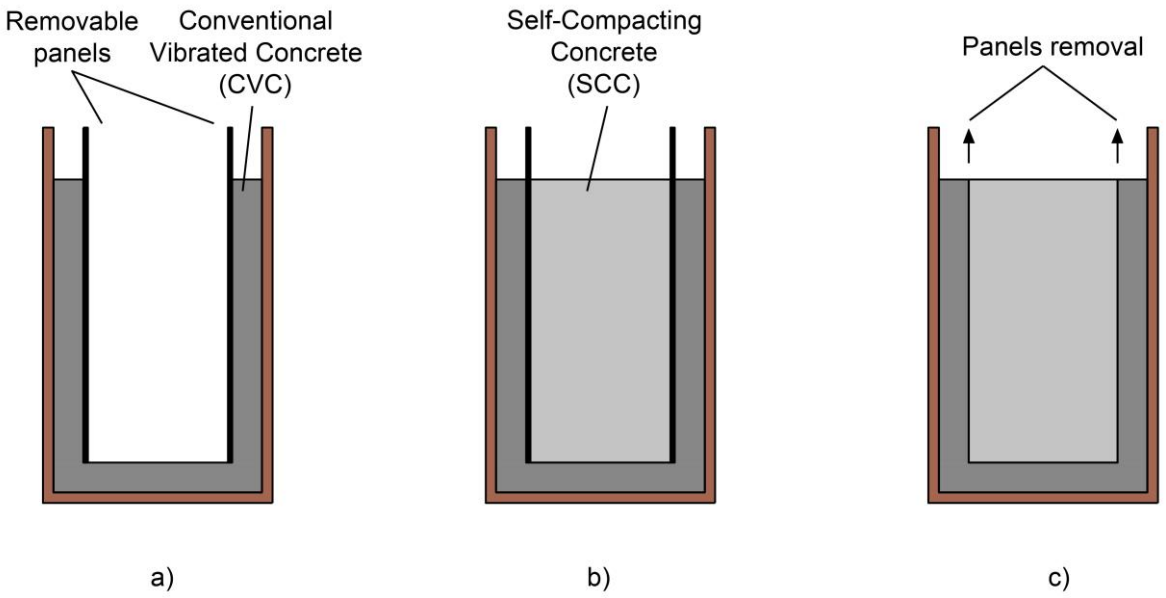

Figure 4 Fresh-on-fresh casting of a composite section composed with a U-shaped external layer: (a) casting and vibration of the external CVC layer with the aid of removable panels, (b) casting of the SCC section core and (c) panels removal.

3 Experimental design

A set of functionally layered elements were cast to illustrate the opportunity to reduce the use of cement through functional layering and to investigate the effects of pour delay on the bond strength of the interface between layers. The elements were composed of an external U-layer of low-porosity cement-intensive CVC and an inner core section of lightweight low-cement SCC. The fresh-on-fresh casting method presented in the previous section is implemented to cast six layered elements with different delays between the castings of the external layer and the core section. Five elements are cast with pour delays of 0, 3, 6, 24 and 48 hours respectively. An additional layered element is produced with a pour delay of 48 hours and a rough interface between the two layers to investigate the effects of the roughness on the effectiveness of the bond. Once the elements had hardened, six cylindrical specimens were cored across the interface between the two materials at different locations to investigate the effects of the fresh-state stresses developing across the interface on the hardened-state bond between two layers. This resulted in 36 bi-layered cylindrical specimens that were tested in direct tension. The material properties of the single mixes were characterised through cube compressive tests and direct tension tests on cylinders cored from single-mix concrete cubes. Three compression tests and three direct tests were performed for each of the seven batches mixed, resulting in 21 tensile tests and 21 compressive tests for material characterization.

3.1 Casting

The fresh-on-fresh casting method presented in section 2 is used here to cast six unreinforced layered elements with different delays Δt between the castings of the external layer and the core section. No reinforcement was embedded in the elements with a view to characterize the effectiveness of the bond between the two layers by coring cylindrical concrete samples across the interface without cutting reinforcement bars. The composite concrete prisms were composed of a 50-mm-thick U-shaped external layer of relatively low-porosity material and a 100-mm-wide core section of relatively high porosity material, with overall dimensions $200 \times 300 \times 300$ mm^3. The target geometry of the layered elements is shown in Figure 5. Five elements, denoted as D0, D3, D6, D24 and D48, are cast with pour delays of 0, 3, 6, 24 and 48 hours respectively. An additional layered element, denoted as D48R, is produced with a pour delay of 48 hours and a rough interface between the two layers to investigate the effects of the roughness of the interface on the effectiveness of the bond.

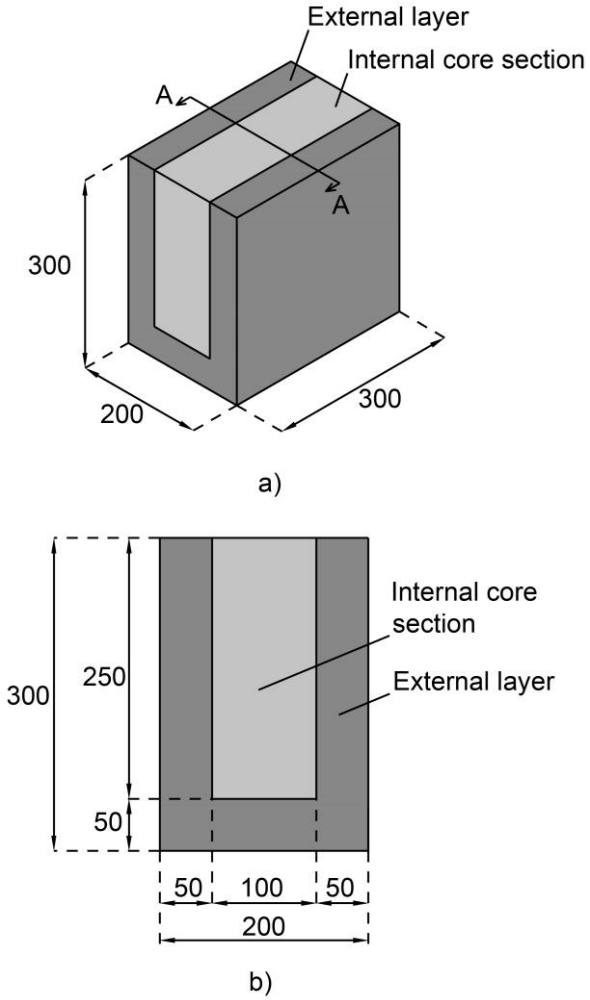

Figure 5 Target geometry for the layered prisms: (a) axonometric view and (b) cross-section AA.

Table 2 Delay Δt between the castings of the external layer and the core section, and treatment of the interface for each specimen.

Element ID	Δt **[hours]**	**Roughened interface**
D0	0	No
D3	3	No
D6	6	No
D24	24	No
D48	48	No
D48R	48	Yes

Rectangular wooden moulds equipped with two vertical removable panels were designed to cast the layered elements (see Figure 6). The internal dimensions of the moulds were 200 × 300 × 350 mm^3. Four vertical

grooves were cut into the internal surfaces of the short sides of the moulds to host the removable panels demarcating three distinct regions (see geometry in Figure 6). The removable panels were acrylic glass sheets with a thickness of 4 mm.

a)

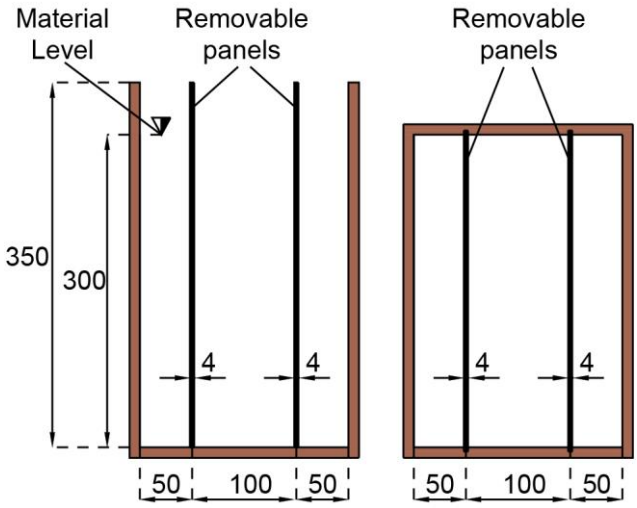

b) c)

Figure 6 (a) Mould equipped with two removable panels, (b) traverse section and (c) plan view.

Figure 7 summarizes the main casting operations. For all the elements, the external U-shaped layer was cast first (see Figure 7a-c). The panels were inserted into the base of the mould to demarcate the regions within which the CVC for the bottom and lateral parts of the external layer was poured (see Figure 7a). To achieve full compaction of the poured material, vibration was applied with the panels in place. Following compaction of the three distinct masses of concrete, the panels were lifted by 50 mm, thereby creating voids that were not

fully filled by the concrete due to its relatively high yield stress (Figure 7b). A gentle vibration was thus applied with the panels in the lifted position to temporarily reduce the yield stress of the material, thereby triggering concrete fluid flow and filling the voids (Figure 7c). This procedure allowed the external layer to be fully compacted with limited and controlled deformations.

The core section SCC was then poured. For element D0, the core material was mixed at the same time as the external mix and poured immediately after compaction of the external CVC layer. For elements D3, D6, D24, D48 and D48R, the core section material was mixed and poured with a time delay Δt of 3, 6, 24, 48 and 48 hours respectively. For elements D0 and D3, the removable panels were removed immediately after pouring of the core section material (see Figure 7d and Figure 7e). This allowed the two external columns of materials to always be supported by either the removable panels or by the confining pressure offered by the core section SCC. By contrast, elements D6, D24, D48 and D48 were obtained by lifting the panels 4 hours after casting of the external CVC layer, that is, prior to casting of the core section material (see Figure 7f and Figure 7g). This allowed the external layer to be supported on setting and the vertical panels to be extracted with ease. For specimen D48R, the three inner surfaces of the external layer were roughened 4 hours after casting following the extraction of the panels. A wired brush was used to expose the aggregates and create a rough interface between the two materials. A summary of the delay between castings of the external layer and the core section, and treatment of the interface for each specimen is provided in Table 2.

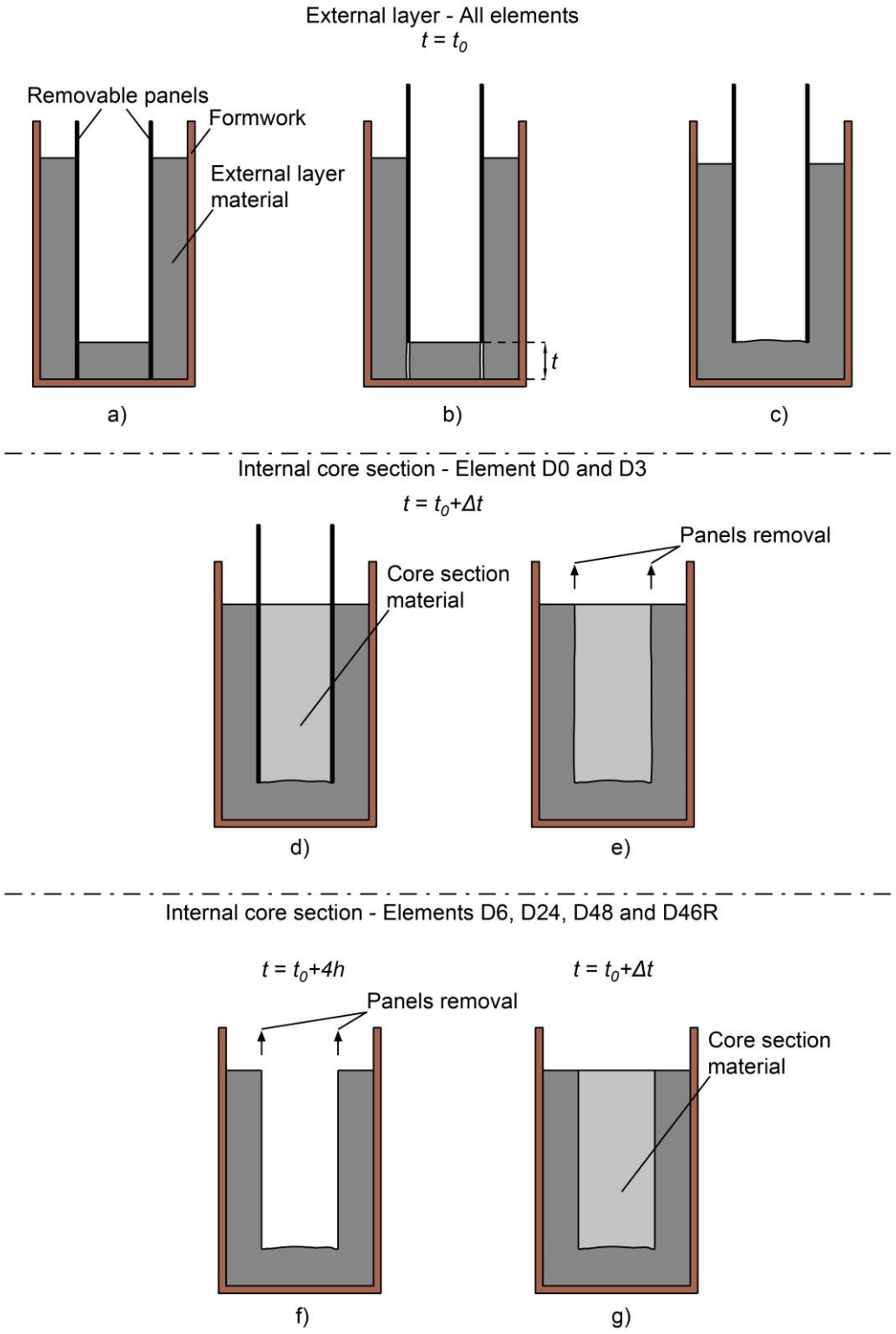

Figure 7 Main casting operations for all of the six elements. Casting of the external layer: (a) pouring of the external layer material, (b) partial lifting of the panels and (c) vibration. Casting of the core section for elements D0 and D3: (d) pouring of the core section material and (e) panels removal. Casting of the core section for elements D6, D24, D48 and D48R: (f) panels removal and (g) pouring of the core section material.

3.2 Materials

The mix compositions of the materials for the external layer and the core section were designed with a view to achieve a significant porosity differential in the hardened state, as well as rheological properties that allowed for effective compaction and limited deformations in the fresh state.

To achieve a significant differential in porosity and, consequently, a significant differential in cement content, water/cement ratios of 0.40 and 0.65 were adopted for the external layer and the core section respectively. Furthermore, foam was used in the internal core material for a further increase in the porosity of the cement paste. This resulted in cement contents of 450 and 277 kg m^{-3} in the external layer and core section respectively. A weight differential of around 400 kg m^{-3} between the two mixes was also obtained by combining the use of foam and lightweight aggregate for the core section material. According to equations (1-1) and (1-2), the adopted materials and cross-section geometry (see Figure 5) allow for cement savings S_C of 16 % and weight savings S_W of 7 %. By using a PCE superplasticizer, typical CVC and SCC workability levels were achieved for the external layer and the core section material respectively.

Table 3 shows the composition for the two mixes. A standard Portland-limestone cement CEM II/A-LL strength class 32.5R complying with European Standard EN 197-1 [39] was used. The maximum particle diameter of the sand and the gravel were 4 mm and 15 mm respectively. Lightweight aggregate made from fly ash with a maximum particle diameter of 8 mm was used. A surfactant based foaming agent was used to introduce foam in the mix and a high-range PCE superplasticizer complying with the European Standard BE 934-2 [40] was used to achieve the desired workability levels. To visually distinguish the two mixes, a red mortar dye based on powdered oxide pigments was used in the mix for the external layer. The densities of the single mix constituents are reported in Table 4.

Table 3 Mix compositions for the external and internal layers.
*Superplasticizer content expressed in terms of % of cement mass

Constituent	**Unit**	**External layer (E)**	**Core section (I)**
Cement	[kg m^{-3}]	450	277
Water	[kg m^{-3}]	180	180
Sand 0/4 mm	[kg m^{-3}]	769	720
Gravel 4/15 mm	[kg m^{-3}]	979	-
Lytag 0/8 mm	[kg m^{-3}]	-	529
Superplasticizer*	[%]	4.2	3.9
Foam	[L m^{-3}]	-	50
Concrete dye	[kg m^{-3}]	8	-

Table 4 Densities of the mix constituents

Constituent	**Density [kg m^{-3}]**
Cement	3200
Water	1000
Sand (0/4 mm)	2600
Gravel 4/15 mm	2600
Lytag 0/8 mm	1500
Superplasticizer	1100
Foam	50
Concrete dye	3000

Two batches of external layer material, denoted as E1 and E2, and five batches of core section material, denoted as I1 to I5, were mixed. A summary of the concrete batches used for the external layers and the core sections of each element is provided in Table 5. The material for the external layer was mixed in a vertical-axis rotational mixer. Cement, sand, gravel and mortar dye were mixed for 2 minutes in order to obtain a homogenous dry blend. The water was then added gradually while the mixer was running and the mix was mixed for an additional 2 min. By contrast, the mix for the core sections was mixed in an inclined drum mixer. The relatively gentle folding action allowed the foam to be blended uniformly without collapsing the foam bubbles. Dry cement, sand and mortar dye were first mixed for 2 minutes. Water was then added while the mixer was running and the resulting mortar was mixed for 2 minutes. Once a homogeneous mortar was obtained, foam was added and the blend was mixed for an additional 2 minutes. The foam was produced by whisking a 3 % strength foaming-agent solution for 2 minutes using a mixer attachment fitted to a power drill.

Lightweight aggregate was finally added and the resulting mix was mixed for 2 minutes. Adding the lightweight aggregate at the end of the mixing processes allowed the collapse of the foam to be minimised.

Table 5 Batches used for six layered-elements.

Element ID	Batches ID	
	External layer (E)	Core Section (I)
D0	E1	I1
D3	E2	I4
D6	E1	I2
D24	E1	I3
D48	E2	I5
D48R	E2	I5

3.3 Rheological and strength measurements

The rheological properties and wet densities of each batch of concrete were measured around 10 minutes after mixing and immediately before casting the layered elements to obtain a reliable assessment of the instantaneous values. The yield stresses of the CVC external layer and SCC core section materials were measured through slump and LCPC-box channel flow tests respectively. For the core section material, the LCPC-box test was preferred to a classic slump flow test as it generally gives more reliable results in the case of SCCs [41]. This is due to the fact that, when the slump flow tests are performed on SCC, the thickness of the sample at flow stoppage is often of the same order as the size of the largest particles [41]. The wet density of the mixes was measured indirectly by weighing a volume of 8 litres of material.

The slump tests were performed in accordance to the European Standard EN 12350-2 [42]. The yield stress τ_0 was then calculated as a function of slump s and wet density ρ through the analytical relationship reported in [43] for slumps in the range of 50 – 250 mm. The LCPC-box channel flow tests were performed according to the procedure defined in [41]. The test measures the ability of a volume of 6 litres of fresh concrete to flow through a wooden box having a length of 120 cm, a width of 20 cm and a height of 15 cm. The spread length L in the box at flow stoppage is measured. The yield stress was then assessed as a function of spread length L and wet density ρ through the analytical expression presented in [41] that has been validated in [41] and [44] against rotational rheometers measurements.

To characterize the compressive and tensile strength of the materials, six 100-mm-cubes were cast for each of the seven batches of concrete (E1, E2, I1-I5). Three of the six cubes cast for each batch were used to characterize the compressive strength while the remaining three cubes were used to characterize the tensile strength.

3.4 Curing, coring and cutting

The layered elements were cast as described in section 3.1 and covered with plastic sheets immediately after casting. When the two materials were poured with a time delay, plastic sheets were applied immediately after casting of the external layer and then temporarily removed to cast the inner core sections. Approximately 48 hours after casting of the core section material, the specimens were demoulded, wrapped in plastic sheets and left to cure for 14 days. Figure 9 shows specimen D0 after curing and demoulding.

The six control cubes cast for each concrete batch were cured in a curing tank. Three of the six specimens were tested in compression following 28 days of curing. The remaining three cubes were extracted from the tank after 14 days of curing to core cylinders with a diameter of 46 mm as illustrated in Figure 8. The cores were wet-drilled between 14 and 18 days after casting using a power coring-machine using a cylindrical diamond coring-tool. The cored cylinders were then tested in direct tension 35 days after casting following the methodology detailed in the next section.

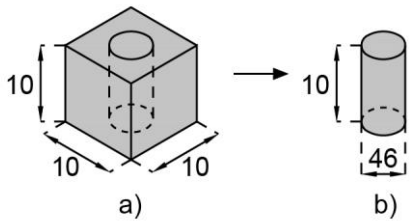

Figure 8 Production of cylinders for the characterization of the material's tensile strength: (a) concrete cube and (b) drilled core cylinder.

Cylindrical cores were also taken across the interface between the two layers of the composite U elements 14 to 18 days after casting of the internal layer (see Figure 10). Two horizontal and two vertical cores were drilled for each of the six U elements. Figure 10 shows the location of the cores. The distance between the axis of a core and the top surface of the layered element is herein referred to as core location depth d. The two horizontal cores were taken at different depths d of 75 and 145 mm to investigate the effects of d on the bond strength between the two materials. To obtain layered cylindrical specimens with a height of 100 mm, the horizontal

and vertical cores were cut as shown in Figure 11a and Figure 11b respectively using a table circular saw. As illustrated in Figure 11, two specimens were obtained from each horizontal core while only one specimen was obtained from each vertical core. This resulted in six layered specimens for each element: two specimens (denoted as V1 and V2) cut from the vertical cores, two (denoted as HT1 and HT2) from the top horizontal core and two (denoted as HB1 and HB2) from the bottom horizontal core.

Figure 9 Specimen D0 after demoulding

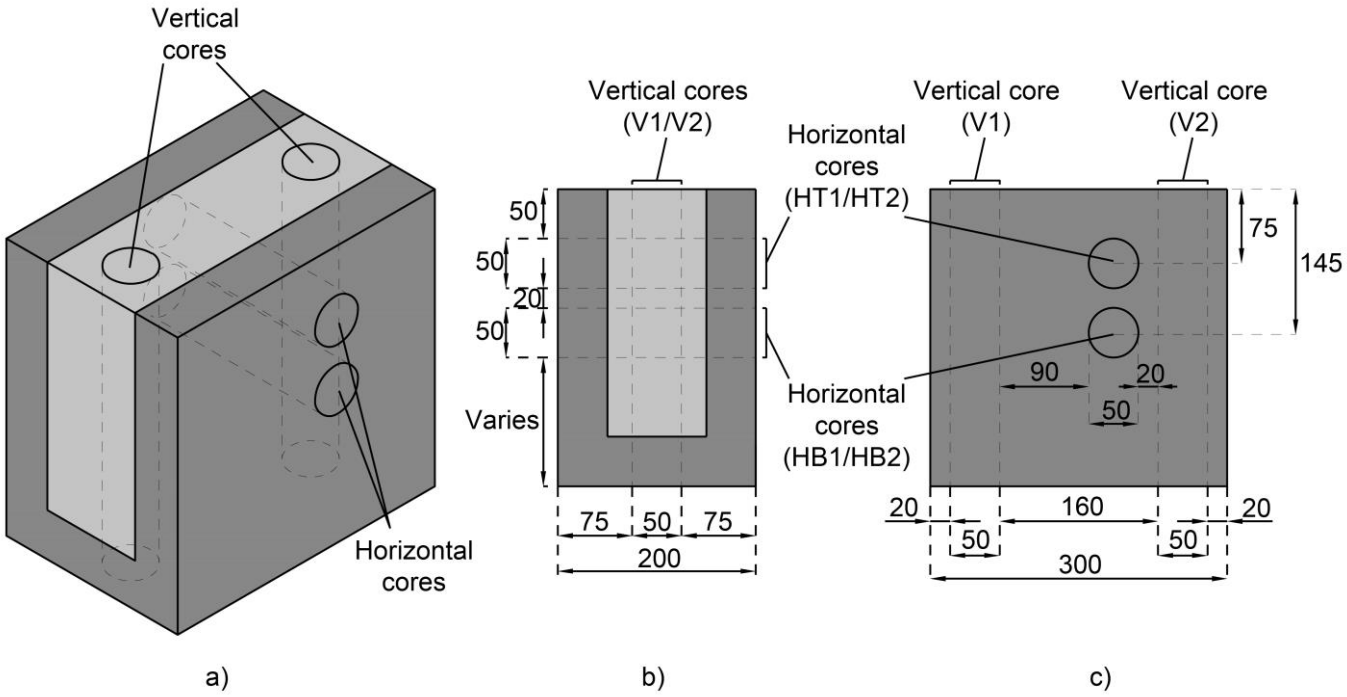

Figure 10 Location of the vertical and horizontal cores: (a) axonometric view of a layered specimen, (b) cross section and (c) lateral view.

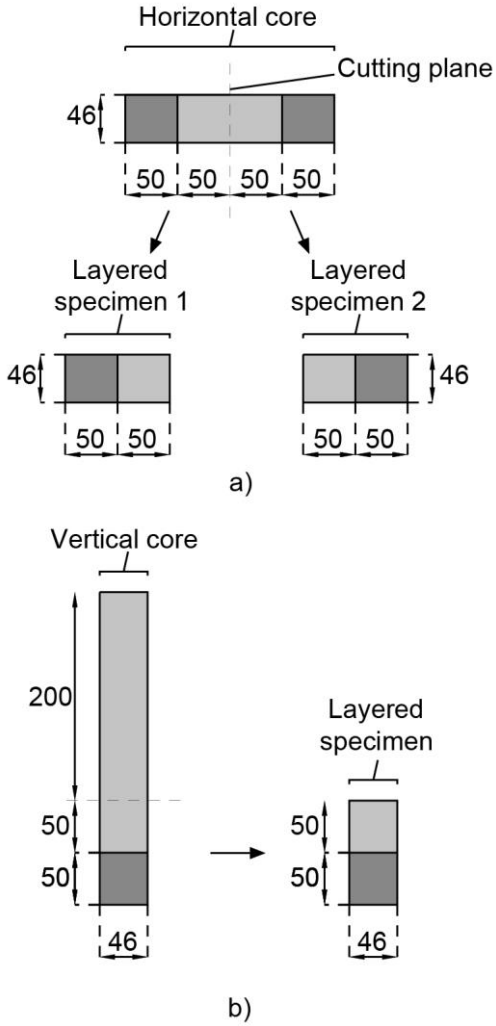

Figure 11 Cutting of (a) horizontal and (b) vertical cores into layered cylindrical specimens with a height of 100 mm.

Following coring, the full prismatic U layered elements were cut in half along the vertical plan parallel to their short side using a table circular saw. This allowed the middle sections of the specimens to be visually inspected and photographed with a high-resolution camera (see Figure 12a). To minimise perspective distortions upstream, the camera was mounted on a tripod such that the focal plane was parallel to the cuts. The residual perspective distortions were then eliminated in a raster graphic editor by marking four reference points on each cross section (see Figure 12b). The maximum thickness $\bar{t}$ of the external layer at the bottom of the element was measured as an indicator of the fresh state deformations of the element (see Figure 12b).

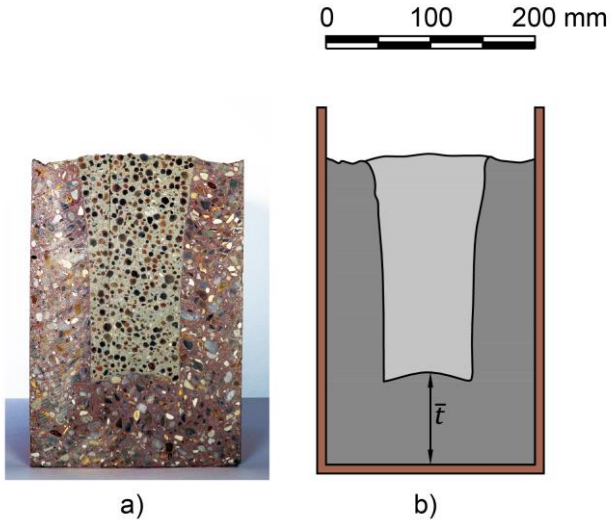

Figure 12 Analysis of the middle cross-section of a layered element: (a) photo and (b) CAD representation.

3.5 Tensile tests

The single-material cylindrical specimens prepared for material characterization and the layered specimens prepared for bond strength assessment were tested in tension in accordance with the European Standard EN 14488-A [45]. To determine the tensile strength of the materials and interfaces, tensile stresses were applied until failure through a hydraulic testing machine with a capacity of 30 kN.

As described previously, all the specimens were cored between 14 and 18 days after casting. Cylindrical steel dollies with a diameter of 46 mm and thickness of 20 mm were manufactured and glued onto the end sections of the cylinders between 20 and 24 days after casting (see Figure 13). A threaded hole was machined on one of the flat surfaces of each dolly to allow for a connection with the testing rig. The dollies were glued to the concrete specimens by using a two-part cold-curing structural adhesive based on epoxy resin with a tensile strength of 10 MPa. Alignment between the steel dollies and the specimens was ensured by using 90-degree steel angle corners on gluing. The glue was left to cure for at least 10 days. The dollies were then connected to the main load frame through double-hinged swivel connections to allow for any residual moment load to be released. The test setup is shown in Figure 14. All the tests were performed 35 days after casting.

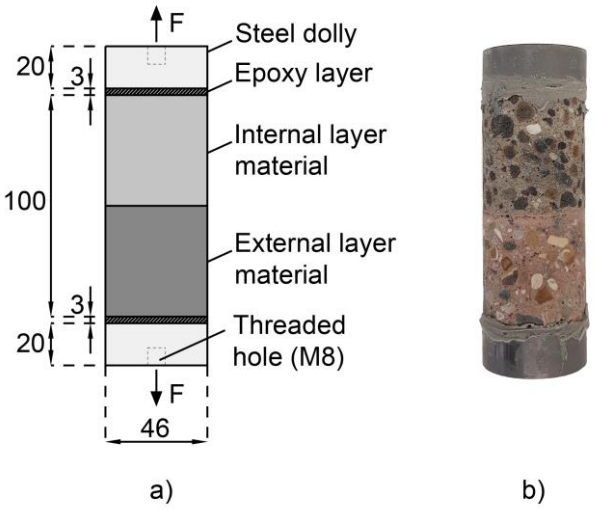

Figure 13 Layered specimen with glued steel dollies: (a) schematic representation and (b) photo.

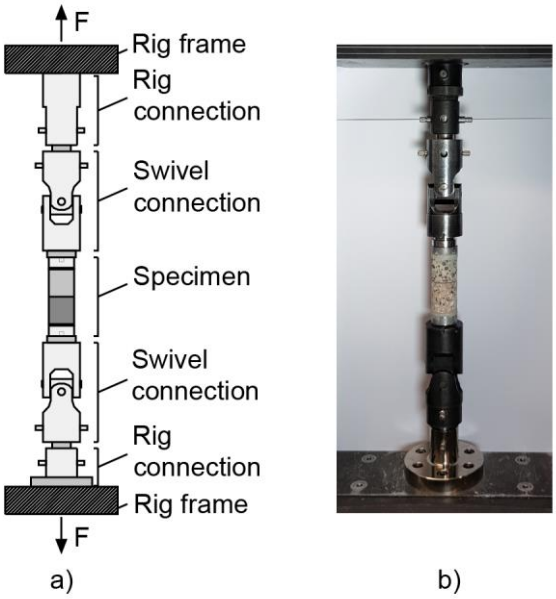

Figure 14 Tensile test set-up

4 Results

4.1 Material properties

Table 6 summarizes the measured fresh and hardened-state material properties. For all the elements, the material of the external layer exhibited a higher wet-density and a higher yield stress than the core section material. A wet density ρ of 2251 and 2255 kg m^{-3} was measured for the two batches E1 and E2 respectively, whereas the five batches I1 to I5 exhibited ρ in the range of 1755 – 1903 kg m^{-3}. The yield stress τ_0 of batches E1 and E2 was 705 and 1087 Pa respectively, while τ_0 in the range of 34 – 57 Pa was measured for batches I1 to I5. The variability of the measured yield stresses might be explained by several factors that influence the rheological behaviour of the material, including the intrinsic variability of the single constituents and the inevitable ambient-temperature differentials for batches mixed and cast at different times.

The external-layer material always exhibited significantly higher cube compressive strengths $f_{c,cub}$ than the material of the internal layer. Batches E1 and E2 had a $f_{c,cub}$ of 54.3 and 40.7 MPa respectively, while a $f_{c,cub}$ in the range of 17.9 – 27.0 MPa was measured for batches I1 to I5. The difference in tensile strength $f_{t,cyl}$ between the materials used for the external layer and core section was generally less evident than the difference in $f_{c,cub}$. Batches E1 and E2 exhibited $f_{t,cyl}$ of 2.6 and 3.1 MPa respectively, whereas $f_{t,cyl}$ in the range of 2.3 – 3.0 MPa was measured for batches I1 to I5.

Table 6 Fresh and hardened state properties of the different batches: wet density ρ, spread length L, slump s, yield stress τ_0, and mean and standard deviation (in brackets) of 28-day cube compressive strength $f_{c,cub}$ and cylinder tensile strength $f_{t,cyl}$.

		Element D0		**Element D3**		**Element D6**	
Measure	**Unit**	**Ext. Layer (E1)**	**Core (I1)**	**Ext. Layer (E2)**	**Core (I4)**	**Ext. Layer (E1)**	**Core (I2)**
ρ	[kg m^{-3}]	2255	1835	2251	1893	2255	1898
L	[mm]	-	715	-	730	-	760
s	[mm]	200	-	170	-	200	-
τ_0	[Pa]	705	34	1087	37	705	38
$f_{c,cub}$	[MPa]	54.3 (2.3)	21.8 (2.0)	40.7 (1.2)	23.2 (0.6)	54.3 (2.3)	22.6 (1.6)
$f_{t,cyl}$	[MPa]	2.6 (0.5)	2.5 (0.3)	3.1 (0.1)	2.6 (0.3)	2.6 (0.5)	2.5 (0.2)
		Element D24		**Element D48**		**Element D48R**	
Measure	**Unit**	**Ext. Layer (E1)**	**Core (I3)**	**Ext. Layer (E2)**	**Core (I5)**	**Ext. Layer (E2)**	**Core (I5)**
ρ	[kg m^{-3}]	2255	1755	2251	1903	2251	1903
L	[mm]	-	610	-	740	-	740
s	[mm]	200	-	170	-	170	-
τ_0	[Pa]	705	57	1087	36	1087	36
$f_{c,cub}$	[MPa]	54.3 (2.3)	17.9 (0.9)	40.7 (1.2)	27.0 (1.0)	40.7 (1.2)	27.0 (1.0)
$f_{t,cyl}$	[MPa]	2.6 (0.5)	2.3 (0.1)	3.1 (0.1)	3.0 (0.3)	3.1 (0.1)	3.0 (0.3)

4.2 Bond between layers in the hardened state

Figure 15a shows the measured tensile strength $f_{t,lay}$ versus pour delay Δt for the layered cylindrical specimens cut from top horizontal cores (HT1 and HT2), bottom horizontal cores (HB1 and HB2) and vertical cores (V1 and V2). Specimens V1 and V2 cut from vertical cores exhibited significantly lower interface tensile strength than the specimens cut from horizontal cores. Of the 12 specimens from vertical cores, 9 broke at the interface on coring and 3 failed at the interface when subjected to tensile stresses lower than 1 MPa. By contrast, specimens cut from horizontal cores exhibited $f_{t,lay}$ in the range of 1 – 3 MPa. This may be attributed to the fact that vertical cores were taken from the top of the specimens. Indeed, due to its rotation, the cylindrical diamond coring-tool transfers shear stresses to the material through its inner surface. When an interface is crossed, the shear stresses transferred by the coring tool determine a torque at the interface. Such torque can be considered proportional to the contact surface between coring tool and concrete and thus to the depth of the core. In the case of vertical cores, the coring tool was deeper into the element than in the case of horizontal cores when it reached the interface between the two materials. This might have caused relatively high torques

that damaged the interface on coring. For this reason, the results obtained from vertical cores were omitted from further discussion. Figure 15a shows that, for Δt greater than or equal to 3 hours, the location depth d at which the horizontal cores were taken had an impact on $f_{t,lay}$. Specimens HB1 and HB2, taken at a d of 145 mm from the top surface, generally exhibited higher strengths than specimens HT1 and HT2, taken at a d of 75 mm.

Three different failure modes were observed for the layered cylinders cut from horizontal cores, namely failure of the interface, the external layer and the internal core material. The relationship between tensile strength $f_{t,lay}$, pour delay Δt and failure mode for layered cylinders cut from horizontal cores is shown in Figure 15b. The plot shows that for Δt longer than 6 hours, all the specimens failed at the interface. For $\Delta t = 0$, i.e. for fresh-on-fresh casting, none of the specimens failed at the interface. For pour delays of 3 and 6 hours, two and three specimens failed at the interface respectively. Of the 7 specimens that did not fail at the interface, 3 exhibited failure of the external-layer material and 4 failure of the core section material. It can also be noted that the results obtained for $\Delta t = 0$ are less scattered than those obtained with a pour delay. Standard errors of 0.09, 0.29, 0.40, 0.19 and 0.25 are obtained for a Δt of 0, 3, 6, 24 and 47 hours respectively.

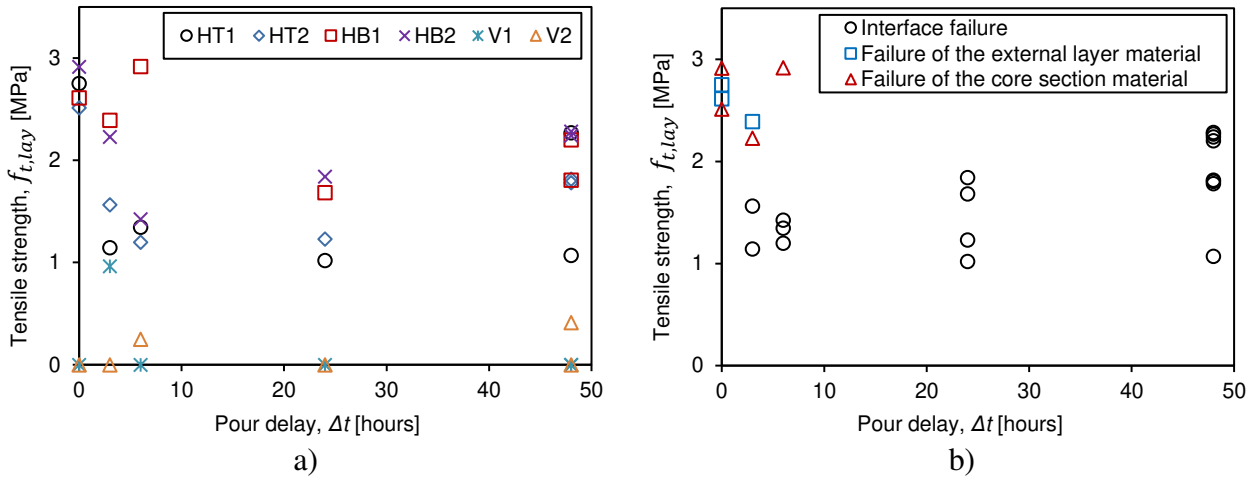

Figure 15 (a) Relationship between tensile strength $f_{t,lay}$ and pour delay Δt for layered specimens cut from top horizontal cores (HT1 and HT2), bottom horizontal cores (HB1 and HB2) and vertical cores (V1 and V2), (b) Relationship between tensile strength $f_{t,lay}$, pour delay Δt and failure mode for layered cylinders cut from horizontal cores.

Figure 16a shows the average tensile strength $f_{t,lay}$ of the layered cylinders versus pour delay Δt. It can be observed that the pour delay has a significant impact on the average tensile strength. The average $f_{t,lay}$ decreases monotonically for Δt of up to 24 hours. In this range, the curve Δt - $f_{t,lay}$ is non-linear. Reductions

in $f_{t,lay}$ of 32, 36 and 46 % of the value obtained for Δt = 0 are observed for a Δt of 3, 6 and 24 hours respectively. A slight increase in average $f_{t,lay}$ is observed for Δt higher than 24 hours. Specifically, $f_{t,lay}$ increases by 20 % between 24 and 48 hours. Figure 16a also shows the average $f_{t,lay}$ obtained for Δt of 48 hours and a rough interface between the layers (element D48R). By roughening the interface, 41 % of the drop in tensile strength due to a pour delay of 48 hours is recovered. The average tensile strength $f_{t,lay}$ of the cylinders is normalised with respect to the tensile strength $f_{t,cyl}$ of the weaker of the two materials to give the normalised average tensile strength, denoted as $\bar{f}_{t,lay}$. In Figure 16b, $\bar{f}_{t,lay}$ is plotted against the pour delay Δt. For increasing Δt in the range of 0 – 24 hours, $\bar{f}_{t,lay}$ follows the same trend as $f_{t,lay}$. By contrast, different trends are observed for Δt in the range of 24 – 48 hours, where an increase in Δt corresponds to an increase in $f_{t,lay}$ and a decrease in $\bar{f}_{t,lay}$. This is because the concrete batch I5, used for the core material of element D48 cast with a Δt of 48 hours, exhibits a significantly higher $f_{t,cyl}$ than the other batches (see Table 6). The decrease in $\bar{f}_{t,lay}$ is almost linear for Δt in the range of 6 – 48 hours.

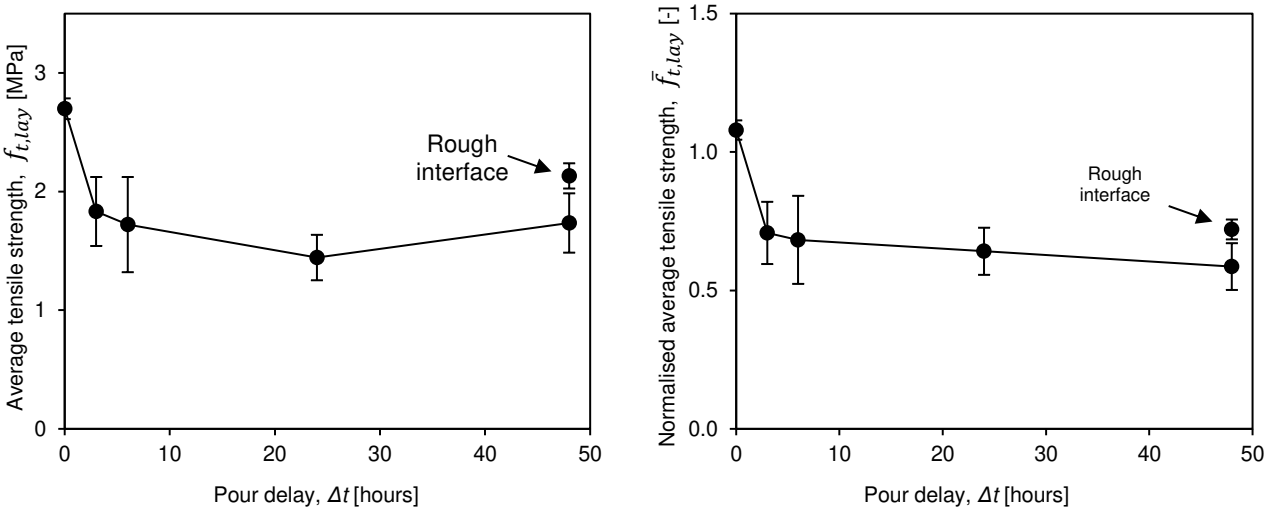

a) b)

Figure 16 (a) Average tensile strength $f_{t,lay}$ and (b) average tensile strength $\bar{f}_{t,lay}$ normalised with respect to the tensile strength $f_{t,cyl}$ of the weaker of the two materials versus pour delay Δt.

4.3 Fresh state deformations

Figure 17 shows the boundary between the two materials and the deformed shape of the middle section of each element. In all the elements, the external layer was significantly thicker at the bottom of the section than at the sides. This can be attributed to a time-dependent creep flow of the heavier materials of the sides towards the bottom part of the formwork. Indeed, creep deformations can take place in fresh concrete even for stress states that do not exceed the yield stress [26,28].

Neither abrupt changes in thickness of the external layer nor macroscopic voids were visually detected in the middle section of element D0. By contrast, two vertical indents were observed in the bottom part of the external layer of all the other elements. The observed intents were approximately rectangular and aligned with the lateral sides of the core section in the horizontal direction. Their thickness was in the range of 3 – 4 mm, while their depth was in the range of 40 – 70 mm. The indents were either empty (see specimen D24 in Figure 17) or partly filled with cement paste of internal section material (see elements D3, D6, D48 and D48R in Figure 17).

The observed indents could be attributed to the combined effects of creep deformations and concrete setting. When the materials are cast with a pour delay, creep flow occurs with the panels in the lifted position (see Figure 7c). Hence, the material flows below the panels. For pour delays greater than or equal to 3 hours, the external layer material around the bottom edge of the panels starts to set prior to removal of the panels. Vertical indents are thus obtained when the panels are lifted. Because of the their relatively small thickness, the indents cannot accommodate the aggregate of the core section material. Thus, the indents are either empty or partly filled by the cement paste of the core section material.

The maximum thickness $\bar{t}$ of the external layer at the bottom of the element was around 50 mm on casting and in the range of 89 – 121 mm in the hardened state. Figure 18 shows the maximum thickness $\bar{t}$, taken as an indicator of the creep deformations developing in the fresh state, as a function of the pour delay Δt. The graph shows that $\bar{t}$ generally increases with increasing Δt. This trend is clearer if the results obtained by using batches E1 and E2 for the external layer are isolated. The authors believe that vertical shift between the curves obtained for batches E1 and E2 is due to a difference in fresh-state creep properties between the two batches. Indeed, it is reasonable to assume that the measured difference in yield stress between the batches E1 and E2 corresponds to a differential in creep properties where the material E1, with a lower yield stress, develops greater creep deformations than the material E2 for a given load level.

In Figure 18, the curve obtained for elements with batch E2 shows a nonlinear trend: around 70 % of the thickness increase obtained for Δt of 24 hours develops for a Δt of 6 hours. This suggests that, for a relatively long Δt, an increase in Δt corresponds to a relatively small increase in $\bar{t}$. This result may be explained by the fact that the ability of the fresh concrete to undergo creep deformations decreases on setting [28].

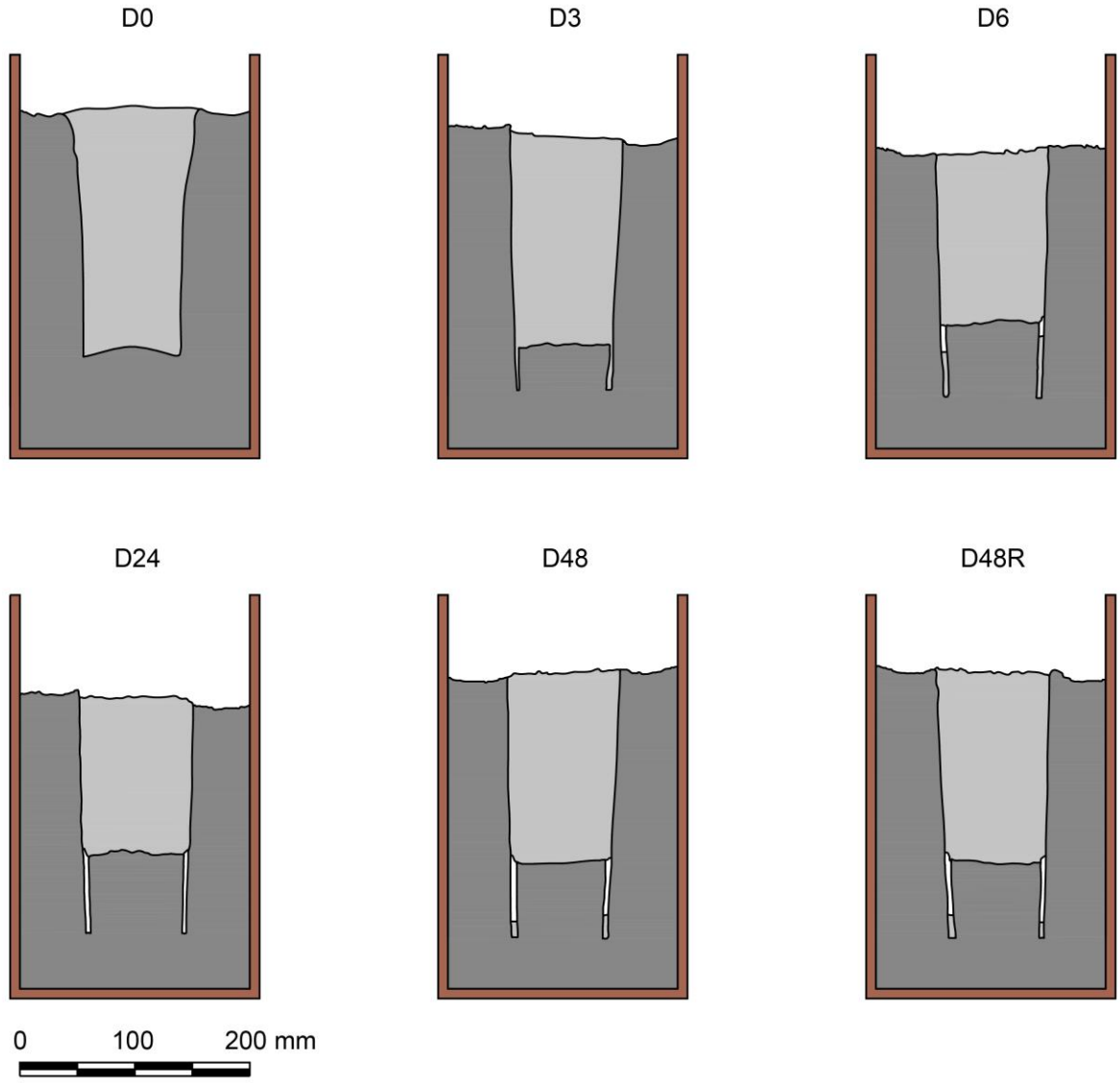

Figure 17 Deformed shape of the middle section of each element.

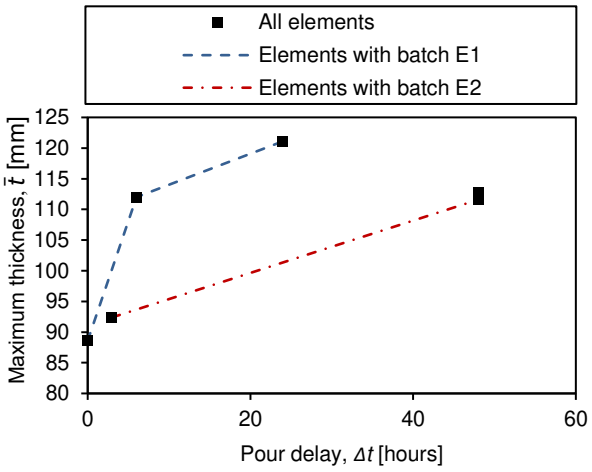

Figure 18 Maximum thickness $\bar{t}$ of the external layer at the bottom of the element as a function of the pour delay Δt

5 Discussion

The results of the tensile tests demonstrate that a tensile bond strength equivalent to the tensile strength of the weaker material can be achieved through fresh-on-fresh casting. Figure 15b shows that none of the specimens cut from horizontal cores of the element cast fresh-on-fresh ($\Delta t = 0$) failed at the interface, meaning that the interface was never the weakest section of the specimens. The delay between the castings of different materials was found to significantly affect the bond between the layers. Figure 16 shows that reductions in interface bond strength of up to more than 40 % are obtained when the materials are cast with a pour delay and that reductions of more than 30 % are already obtained for a pour delay of 3 hours. Hence, the physical and chemical changes taking place within the first 3 hours after casting of the older material play a key role in the strength reduction associated with a pour delay.

In Figure 19, the relationship between normalised average tensile strength $\bar{f}_{t,lay}$ and pour delay Δt, presented in Figure 16b, is combined with the rate of evolution of heat of a Portland cement paste obtained from other authors [46]. The rate of evolution of hydration heat can be considered as an indicator of the rate of hydration of the material [9]. The heat evolution rate reported in Figure 19 was obtained for a paste with water/cement ratio of 0.4, corresponding to the water/cement ratio used here for the external layer material. Hence, it was taken as representative of the rate of hydration of the external layer. Figure 19 indicates that there are three peaks in the rate of hydration in the first two days after casting [9]. The first peak is higher than the others but has a significantly shorter duration. It corresponds to the initial hydration of the surface of the cement particles, largely involving tricalcium aluminate (C_3A), which does not determine setting. This peak is followed by the so-called dormant period: a period of one-two hours during which the hydration rate is very low and the material is workable. Following the dormant period, the rate of hydration increases slowly and reaches a peak at the age of about 10 hours. In this phase, the products of hydration of individual grains of cement (silicates and aluminates) come into contact with one another, thereby causing setting. Following this second peak, the hydration rate slows down over a long period as the diffusion of water through the pores in the hydration product becomes the controlling factor [47]. A third peak is observed at the age of about 30 hours, due to a renewed reaction of C_3A following the exhaustion of gypsum [9].

Figure 19 shows that, for a Δt of 3 hours, the material of the external layer material has started to set when it comes into contact with the material of the core section. It can be observed that, although the majority of the hydration reactions have not yet developed in the external layer within the first 3 hours after casting, most of the reduction in strength observed for a Δt of 48 hours is already obtained for a Δt of 3 hours. This suggests that the stiffening of the older material due to the combined effects of thixotropy and hydration has a greater impact on the interface bond strength than the overall development of hydration reactions. A possible explanation for this is that stiffening of the older layer prevents intermixing, thereby causing a reduction in actual contact surface between the two materials and thus a local increase in porosity. Consequently, a plane of weakness is obtained. These findings are in line with the results of previous studies conducted on SCCs to establish the relationship between pour delays of up to 3 hours and mechanical performance of cold joints in elements with homogeneous concrete composition [23,24,48]. These studies showed that, within the first 3 hours, the bond strength of the interfaces generally decreases with increasing delay time due to a thixotropy-induced increase in stiffness of the first layer that prevents effective intermixing when the second layer is poured [23,24,48].

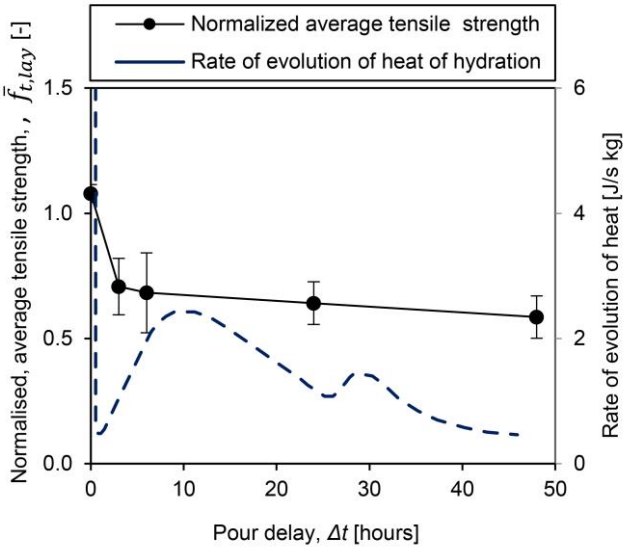

Figure 19 Composite graph: i) average tensile strength $\bar{f}_{t,lay}$ of the layered elements normalised with respect to the tensile strength $f_{t,cyl}$ of the weaker of the two materials versus pour delay Δt, and ii) Rate of evolution* of heat of Portland cement with a water/cement ratio of 0.4 [46]. *The first peak of 3200 J/s kg is off the diagram

Figure 16 shows that by roughening the interface of the older layers prior to casting of the new ones, around 40 % of the drop in tensile strength due to a pour delay of 48 hours can be recovered. This demonstrates that, although beneficial, roughening of the interfaces in fresh-on-hardened casting does not allow the bond strength obtained with fresh-on-fresh casting to be achieved.

The tensile tests also demonstrated that the bond between two different materials cast with a pour delay varies with the considered location. Figure 15 illustrates that, when the two materials are cast with a pour delay, the horizontal specimens taken at a depth d of 145 mm generally exhibited a higher strength than the specimens taken at a d of 75 mm. A possible explanation is that the porosity of the interface decreases with the depth d. It is reasonable to assume that the ability of the newer material to fill all the voids at the interface is proportional to the pressure it exerts on the older material, which in turn grows with increasing depth d.

Practical applications can be envisaged where the structural behaviour of functionally layered sections relies on the mechanical performance of horizontal and/or vertical interfaces. If, for example, an external low-permeability layer is designed to boost the durability performance of a column, the bond strength of the resulting vertical interfaces is expected to affect both the serviceability and the ultimate limit state performance in bending. Similarly, when horizontal layers are introduced to optimize the performance of beams and slabs subjected to bending, the bond strength behaviour of the horizontal interfaces is expected to influence the overall performance of the member. More research is thus needed to better understand the association between layers orientation and interface bond strength.

The analysis of the fresh state deformations demonstrates that the proposed fresh-on-fresh casting method is an effective way to produce functionally layered elements with a low-porosity U-shaped external layer. If the method is applied to cast the materials fresh-on-fresh (i.e. with $\Delta t = 0$), a well-compacted layered section is obtained having an external layer with no abrupt changes in thickness. Hence, the method can be readily used for the efficient production of layered concrete elements. By contrast, if the method is employed to cast the two materials with a time delay, macroscopic voids and abrupt changes in the thickness of the external layer are obtained. The proposed fresh-on-fresh casting method has been designed and verified for the specific proof-of-concept cross-sectional geometry reported in Figure 5b. However, the fundamental principles underlying this method could be applied to design analogue techniques to cast different cross-sectional geometries. If, for example, larger elements were to be designed, adequate compaction and control of the fresh state deformations could in principle be achieved by appropriate tailoring of the fresh state properties of the materials.

6 Conclusions

An original fresh-on-fresh casting method is proposed to realise functionally layered concrete sections composed of an external U-shaped durability layer of low porosity concrete and a rectangular lightweight bulk core section. Such a design concept can be adopted to minimise the use of cement and to reduce the self-weight of precast concrete beams. This work makes a fundamental contribution to research on functionally layered concrete by demonstrating the proof-of-concept and studying for the first time the effects of delays between successive pours on the bond between different concrete mixes. The relationship between pour delay and effectiveness of the bond between layers is then established by coring cylindrical samples across interfaces and testing the cylindrical cores in tension.

The following conclusions can be drawn:

- When the mix selection for concrete beams is driven by durability requirements for conventional mixes, cement savings of more than 25 % can be achieved through functional layering. Cement-intensive mixes can be used only in the concrete cover, where the ingress of aggressive substances represents a threat to the durability of the element, thereby saving cement in the core of the element.
- If lightweight mixes are used in the bulk core section of a functionally layered precast beam, weight savings of more than 30 % can be achieved. Consequently, dead loads are reduced, more slender elements are designed, and less material is required.
- Composite precast beams composed of an external U-layer of low-porosity cement-intensive Conventional Vibrated Concrete (CVC) and a lightweight core section of Self-Compacting Concrete (SCC) can be cast fresh-on-fresh through the aid of removable panels that demarcate the layers on casting. Such an approach was validated by realising a prototype prismatic U-layer element that represents a proof-of-concept for future production.
- Good tensile bond between two layers of different concrete mixes can be achieved through fresh-on-fresh casting. Hence, fresh-on-fresh casting represents a promising technique to realise tailored, low-carbon concrete members with an improved mechanical performance.
- For two different materials cast at different times, the delay between the castings significantly affects the tensile bond between layers. Reductions in interface bond strength of up to more than 40 % can be obtained when the materials are cast with a pour delay of 48 hours. It was also shown that interface bond strength reductions of more than 30 % can already be obtained for a pour delay of 3 hours. Hence, the physical and chemical changes taking place in the older material within the first 3 hours after casting

play a key role in the strength reduction associated with a pour delay. This suggests that the early-age stiffening of the older material due to the combined effects of thixotropy and hydration has an impact on the interface bond strength.

- Up to 40 % of the reduction in interface tensile strength due to a pour delay can be recovered by roughening the surface of the older layer prior to casting of the new one. This demonstrates that, although beneficial, roughening of the interfaces in fresh-on-hardened casting does not allow the bond strength obtained with fresh-on-fresh casting to be achieved.
- If two different materials are cast with a pour delay, the effectiveness of the bond between the two layers varies with the considered location. The results of the tensile tests performed on horizontal cores through a vertical layer suggest that the hardened-state bond strength increases with an increase in the pressure exerted by the newer material on the older one in the fresh-state. This might be explained by the fact that the ability of the newer material to fill all the voids at the interface grows with the pressure it exerts on the older material. Hence, an increase in compressive pressure across the interface in the fresh-state corresponds to a decrease in porosity and thus an increase in bond strength in the hardened state.

Acknowledgements

The authors would like to acknowledge the financial support of EPSRC - the Engineering and Physical Sciences Research Council (UK) – through the Fellowship 'Tailored Reinforced Concrete Infrastructure: Boosting the Innate Response to Chemical and Mechanical Threats' [Project reference number: EP/N017668/1]. The authors also wish to extend their sincere thanks to Lorna Roberts and the staff of the University of Cambridge Structures Research Lab for their invaluable assistance in carrying out the experimental program previously reported. Additional data related to this publication is available at the University of Cambridge's institutional data repository: https://doi.org/10.17863/CAM.50121.

References

[1] Boden T, Andres R, Marland G. Global, regional, and national fossil-fuel CO2 emissions. Oak Ridge, Tenn., U.S.A.: Carbon Dioxide Information Analysis Center, Oak Ridge National Laboratory, U.S. Department of Energy; 2013. doi:10.3334/CDIAC/00001_V2013.

[2] Heinz P, Herrmann M, Sobek W. Production method and application of functionally graded components in construction (Herstellungsverfahren und Anwendungsbereiche für funktional gradierte Bauteile im Bauwesen). Stuttgart: Fraunhofer IRB Verlag; 2012.

[3] Nes LG, Øverli JA. Structural behaviour of layered beams with fibre-reinforced LWAC and normal density concrete. Mater Struct 2016;49:689–703. doi:10.1617/s11527-015-0530-9.

[4] Bajaj K, Shrivastava Y, Dhoke P. Experimental study of functionally graded beam with fly ash. J Inst Eng Ser A 2013;94:219–27. doi:10.1007/s40030-014-0057-z.

[5] Torelli G, Fernández MG, Lees JM. Functionally graded concrete: Design objectives, production techniques and analysis methods for layered and continuously graded elements. Constr Build Mater 2020;242:118040. doi:10.1016/J.CONBUILDMAT.2020.118040.

[6] Ahmad S. Reinforcement corrosion in concrete structures, its monitoring and service life prediction—a review. Cem Concr Compos 2003;25:459–71. doi:10.1016/S0958-9465(02)00086-0.

[7] Lepech M, Li VC. Water permeability of cracked cementitious composites. Adv Civ Eng Mater Res Lab - Univ Michigan, USA 2005.

[8] Maalej M, Li VC. Introduction of strain-hardening engineered cementitious composites in design of reinforced concrete flexural members for improved durability. ACI Struct J 1995;92:167–76. doi:10.14359/1150.

[9] Neville AM. Properties of concrete. 4th and final edition. 1995.

[10] Wen X, Tu J, Gan W. Durability protection of the functionally graded structure concrete in the splash zone. Constr Build Mater 2013;41:246–51.

[11] Papadakis VG. Effect of supplementary cementing materials on concrete resistance against carbonation and chloride ingress. Cem Concr Res 2000;30:291–9. doi:10.1016/S0008-8846(99)00249-5.

[12] Elliott KS. Precast concrete structures. CRC Press; 2016.

[13] Teychenné DC, Franklin RE, Erntroy HC, Marsh BK. Design of normal concrete mixes. HM Stationery Office; 1975.

[14] Silfwerbrand J. Concrete bond in repaired bridge decks. Concr Int 1990;12:61–6.

[15] Denariè E, Brühwiler E. Tailored composite UHPFRC-concrete structures. Meas. Monit. Model. Concr. Prop. An Int. Symp. Dedic. to Profr. Surendra P. Shah, Northwest. Univ. U.S.A., Dordrecht: Springer Netherlands; 2006, p. 69–75. doi:10.1007/978-1-4020-5104-3_8.

[16] Graybeal B. Design and construction of field-cast UHPC connections. United States. Federal Highway Administration; 2014.

[17] Bull DK, Park R. Seismic resistance of frames incorporating precast prestressed concrete beam shells. PCI J 1986;31:54–93.

[18] fib. Model Code 2010 - Final draft, vol. 1. Fib Bull 2012;1.

[19] fib. Model Code 2010 - Final draft, vol. 2. Fib Bull 2012;2.

[20] Chandra Kishen JM, Rao PS. Fracture of cold jointed concrete interfaces. Eng Fract Mech 2007;74:122–31. doi:10.1016/J.ENGFRACMECH.2006.01.017.

[21] Li G, Xie H, Xiong G. Transition zone studies of new-to-old concrete with different binders. Cem Concr Compos 2001. doi:10.1016/S0958-9465(01)00002-6.

[22] Volz JS, Olson CA, Oesterle RG, Gebler SH. Are they pour lines or cold joints? Concr Constr Mag 1997.

[23] Megid WA, Khayat KH. Bond strength in multilayer casting of self-consolidating concrete. ACI Mater J 2017;114:467–76. doi:10.14359/51689597.

[24] Roussel N, Cussigh F. Distinct-layer casting of SCC: The mechanical consequences of thixotropy. Cem

Concr Res 2008;38:624–32. doi:10.1016/J.CEMCONRES.2007.09.023.

[25] Torelli G, Lees JM. Fresh state stability of vertical layers of concrete. Cem Concr Res 2019;120:227–43. doi:10.1016/J.CEMCONRES.2019.03.006.

[26] Coussot P. Yield stress fluid flows: A review of experimental data. J Nonnewton Fluid Mech 2014;211:31–49. doi:10.1016/j.jnnfm.2014.05.006.

[27] Tattersall GH, Banfill PFG. The Rheology of Fresh Concrete. Boston: Pitman Books Limited; 1983.

[28] Banfill PFG. Rheology of fresh cement and concrete. Rheol. Rev. 2006, The British Society of Rheology; 2006, p. 61–130.

[29] Roussel N. Understanding the Rheology of Concrete. Woodhead Publishing; 2012.

[30] Petit J-Y, Khayat KH, Wirquin E. Coupled effect of time and temperature on variations of yield value of highly flowable mortar. Cem Concr Res 2006;36:832–41. doi:10.1016/J.CEMCONRES.2005.11.001.

[31] Petit J-Y, Khayat KH, Wirquin E. Coupled effect of time and temperature on variations of plastic viscosity of highly flowable mortar. Cem Concr Res 2009;39:165–70. doi:10.1016/J.CEMCONRES.2008.12.007.

[32] Tattersall GH, Baker PH. The effect of vibration on the rheological properties of fresh concrete. Mag Concr Res 1988;40:79–89. doi:10.1680/macr.1988.40.143.79.

[33] Tattersall GH, Baker PH. An investigation on the effect of vibration on the workability of fresh concrete using a vertical pipe apparatus. Mag Concr Res 1989;41:3–9. doi:10.1680/macr.1989.41.146.3.

[34] Maalej M, Ahmed SFU, Paramasivam P. Corrosion durability and structural response of functionally-graded concrete beams. J Adv Concr Technol 2003;1:307–16. doi:10.3151/jact.1.307.

[35] Roesler J, Paulino G, Gaedicke C, Bordelon A, Park K. Fracture behavior of functionally graded concrete materials for rigid pavements. Transp Res Rec J Transp Res Board 2007;2037:40–9.

[36] Li Q, Xu S. Experimental investigation and analysis on flexural performance of functionally graded composite beam crack-controlled by ultrahigh toughness cementitious composites. Sci China Ser E Technol Sci 2009;52:1648–64. doi:10.1007/s11431-009-0161-x.

[37] Naghibdehi MG, Mastali M, Sharbatdar MK, Naghibdehi MG. Flexural performance of functionally graded RC cross-section with steel and PP fibres. Mag Concr Res 2014;66:219–33. doi:10.1680/macr.13.00248.

[38] Liu X, Yan M, Galobardes I, Sikora K. Assessing the potential of functionally graded concrete using fibre reinforced and recycled aggregate concrete. Constr Build Mater 2018;171:793–801. doi:10.1016/J.CONBUILDMAT.2018.03.202.

[39] European Committee for Standardization. EN 197-1:2011 – Cement – Part 1: Composition, specifications and conformity criteria for common cements 2011.

[40] European Committee for Standardization. EN 934-2 - Admixtures for concrete, mortar and grout - Part 2: Concrete admixtures; definitions, requirements, conformity, marking and labelling 2009.

[41] Roussel N. The LCPC box: a cheap and simple technique for yield stress measurements of SCC. Mater Struct 2007;40:889–96. doi:10.1617/s11527-007-9230-4.

[42] European Committee for Standardization. EN 12350-2 Testing fresh concrete. Slump-test 2009.

[43] Roussel N. Correlation between yield stress and slump: comparison between numerical simulations and concrete rheometers results. Mater Struct 2006;39:501. doi:10.1617/s11527-005-9035-2.

[44] Nguyen TLH, Roussel N, Coussot P. Correlation between L-box test and rheological parameters of a homogeneous yield stress fluid. Cem Concr Res 2006;36:1789–96. doi:10.1016/J.CEMCONRES.2006.05.001.

[45] European Committee for Standardization. EN 14488-4 - Testing sprayed concrete - Part 4: Bond strength of cores by direct tension 2005.

[46] Struble L, Livesey P, Strother PD, Bye G. Portland cement: composition, production and properties. Third Edit. London, UK: ICE Publishing; 2011. doi:10.1680/pc.36116.001.

[47] Brunauer S, Skalny J, Odler I, Yudenfreund M. Hardened portland cement pastes of low porosity: VII. Further remarks about early hydration. Composition and surface area of tobermorite gel. Summary. Cem Concr Res 1973;3:279–93. doi:https://doi.org/10.1016/0008-8846(73)90031-8.

[48] Assaad JJ, Issa CA. Preliminary study on interfacial bond strength due to successive casting lifts of self-consolidating concrete – Effect of thixotropy. Constr Build Mater 2016;126:351–60. doi:10.1016/J.CONBUILDMAT.2016.09.049.